

Determination of Anomalous Superexchange in MnCl_2 and Its Graphite Intercalation Compound

David G. Wiesler

Department of Physics, The George Washington University, Washington, D.C. 20052

Masatsugu Suzuki and Itsuko S. Suzuki

Department of Physics, State University of New York, Binghamton, New York 13902-6000

Nicholas Rosov

Reactor Radiation Division, National Institute of Standards and Technology, Gaithersburg, Maryland 20899

(Received 21 February 1995)

The low-temperature magnetic structure of MnCl_2 graphite intercalation compound has been studied by neutron diffraction. Magnetic peaks occur at wave vectors incommensurate with the MnCl_2 and graphene sublattices. The in-plane spin configuration is explained by an exchange Hamiltonian that includes three shells of nearest neighbors in the plane. The nearest-neighbor exchange is ferromagnetic but anomalously weak, and the magnetic behavior is dominated instead by the antiferromagnetic third-neighbor interaction. The exchange parameters are used to explain the spin configuration of bulk MnCl_2 after adding an interplanar coupling.

PACS numbers: 75.25.+z, 68.65.+g, 75.30.Kz, 75.40.-s

MnCl_2 belongs to the CdCl_2 class of layered materials, in which divalent metal ions lie in close-packed triangular layers, separated by two layers of Cl^- ions. The magnetic properties of most of the transition-metal dichlorides were vigorously investigated several decades ago. Of the $3d$ metal dichlorides, those with greater than half-filled d orbitals exhibit metamagnetism, characterized by a ferromagnetic alignment of spins within the layers and a much weaker antiferromagnetic coupling between adjacent layers. Those with less than half-filled d orbitals generally exhibit antiferromagnetism within the planes [1]. MnCl_2 represents an intermediate case, and despite extensive study [1–4] the origins of its magnetic structure are still uncertain.

Two features, in particular, have escaped explanation. First, MnCl_2 shows two Néel temperatures, $T_{N1} = 1.96$ K and $T_{N2} = 1.81$ K, both of them quite low when one considers the large magnetic moments ($S = 5/2$) of the Mn^{2+} ions. Other transition-metal dichlorides exhibit a single ordering at much higher temperatures (16 K for CrCl_2 [5], 24 K for FeCl_2 [6], 25 K for CoCl_2 [7], and 52 K for NiCl_2 [8]), despite smaller moments. Second, the two antiferromagnetic phases (between T_{N1} and T_{N2} and below T_{N2}) are characterized by very large unit cells (60 and 90 spins, respectively) that have hampered efforts to understand the structure completely.

The spin Hamiltonian can be simplified by intercalation, which cuts (or dramatically reduces) the magnetic coupling between neighboring layers while preserving the in-plane structure. We report a neutron diffraction study of MnCl_2 -intercalated graphite. We find that the low-temperature spin structure corresponds to that of an incommensurate helimagnet with the spins confined to the intercalate plane. The configuration can be explained only

by including third-neighbor intraplanar interactions in the exchange Hamiltonian. Surprisingly, the near-neighbor coupling is ferromagnetic, despite MnCl_2 graphite intercalation compound's (GIC's) negative Curie-Weiss temperature [9]. More surprisingly, third neighbors dominate the spin Hamiltonian. The magnetic diffraction pattern is similar to that of bulk MnCl_2 , and we have used this similarity to find a set of in-plane exchange parameters that simultaneously explains both data sets. Our work represents the first time that graphite intercalation has been exploited for such a purpose. To our knowledge, it is also the first case reported for an insulator in which the third-neighbor superexchange coupling is likely larger than that of both first and second neighbors.

MnCl_2 GIC samples were prepared from powdered anhydrous MnCl_2 and Kish graphite by the usual methods [9]. To increase the sample size, thirty pieces of these GICs were stacked together on Al foil. The resulting crystal texture had a c -axis mosaic spread of 10° and random orientation in the a - b plane. It consisted of a mixture of stage-1 and stage-2 GIC. Elastic neutron scattering experiments were performed on the BT-2 and BT-9 triple-axis spectrometers at NIST, using neutron wavelengths of 2.433 Å and 2.352 Å, respectively, with the analyzer set for zero energy transfer. The longitudinal resolution was much narrower than all magnetic peaks, and the energy resolutions (>1 meV) were sufficiently large to integrate over all critical scattering. Low temperatures were provided by a ^3He cryostat and a dilution refrigerator.

The top panel in Fig. 1 shows the reciprocal lattice of MnCl_2 GIC. The graphene lattice is defined by reciprocal lattice vectors \mathbf{a}_G^* and \mathbf{b}_G^* (2.952 \AA^{-1}), and \mathbf{a}^* and \mathbf{b}^* are reciprocal lattice vectors of the Mn^{2+} lattice. $|\mathbf{a}^*| = 1.965 \text{ \AA}^{-1}$, essentially the same as for pristine MnCl_2

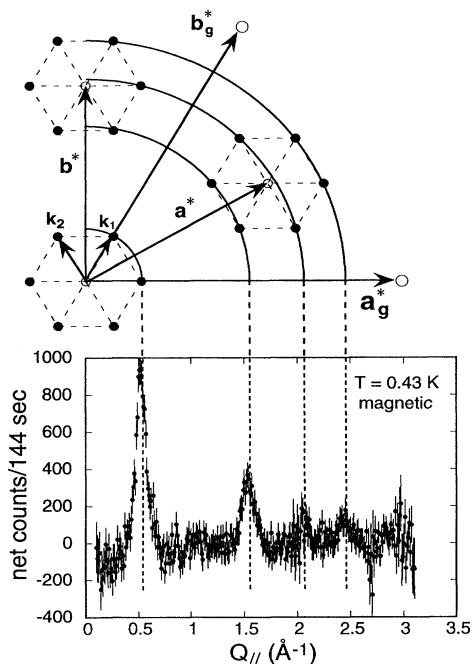


FIG. 1. Top: Schematic reciprocal lattice plane for MnCl_2 GIC. Large open circles are nuclear reflections from the graphite, small open circles are nuclear reflections from the MnCl_2 layer, and closed circles are magnetic reflections. Bottom: Magnetic scattering at $T = 0.43$ K along $[hk0]$.

[3], indicating that intercalation preserves the in-plane structure of MnCl_2 .

The low-temperature magnetic scattering is shown in the bottom panel of Fig. 1, generated by subtracting a scan at 14.85 K, well above the ordering temperature of 1.2 K [10,11], from an identical scan at 0.43 K [12]. These peaks correspond to the magnetic reciprocal lattice shown by closed circles in the top panel. The principal magnetic wave vector \mathbf{k}_1 is indexed to the intercalate lattice as $\text{Mn}(0.153, 0.153)$; it is incommensurate with both the Mn^{2+} and the graphene sublattices. There is no modulation of the magnetic intensity perpendicular to the a - b planes, indicating that it is purely two dimensional.

In order to explain these data, we assume a Hamiltonian consisting of exchange terms and dipole-dipole interactions. This can be written as a Fourier sum [13]:

$$\mathcal{H} = - \sum_{\mathbf{q}} J(\mathbf{q}) \mathbf{S}_{\mathbf{q}} \cdot \mathbf{S}_{-\mathbf{q}} + \sum_{\mathbf{q}} \sum_{\alpha\beta} \mathbf{S}_{\mathbf{q}}^{\alpha} D^{\alpha\beta} \mathbf{S}_{-\mathbf{q}}^{\beta}, \quad (1)$$

where $\mathbf{S}_{\mathbf{q}} = N^{-1/2} \sum_i \mathbf{S}_i e^{-i\mathbf{q} \cdot \mathbf{R}_i}$, $J(\mathbf{q}) = \sum_{j(\neq i)} J(\mathbf{R}_{ij}) \times e^{-i\mathbf{q} \cdot \mathbf{R}_{ij}}$, and where

$$\mathbf{D}^{\alpha\beta}(\mathbf{q}) = \frac{1}{2} (g\mu_B)^2 \sum_{j(\neq i)} R_{ij}^{-3} \left[\delta^{\alpha\beta} - 3 \frac{R_{ij}^{\alpha} R_{ij}^{\beta}}{R_{ij}^2} \right] e^{i\mathbf{q} \cdot \mathbf{R}_{ij}} \quad (2)$$

is the Fourier sum of the dipole coupling. $J(\mathbf{R}_{ij})$ is the exchange coupling between spins \mathbf{S}_i and \mathbf{S}_j , and the indices α and β represent Cartesian coordinates x , y , and

z . The spins in MnCl_2 GIC are known from electron spin resonance measurements to exhibit easy-plane anisotropy [10]; we approximate this by confining the spins to the intercalate plane.

The incommensurate spin structure suggests a helimagnetic configuration [14]: $\mathbf{S}_j = S[\cos(\boldsymbol{\tau} \cdot \mathbf{R}_j)\hat{\mathbf{x}} + \sin(\boldsymbol{\tau} \cdot \mathbf{R}_j)\hat{\mathbf{y}}]$. The ground-state energy per spin U_G is then

$$U_G = -S^2[J(\boldsymbol{\tau}) - \frac{1}{2}\{D^{xx}(\boldsymbol{\tau}) + D^{yy}(\boldsymbol{\tau})\}]. \quad (3)$$

We have split $J(\mathbf{q})$ into shells over first, second, and third neighbors in the plane— J_0 , J_1 , and J_2 —and between neighboring planes, J' .

The absence of intensity modulation along \mathbf{c}^* implies $J' \approx 0$. If we consider the dipole coupling [$\gamma_D \equiv (g\mu_B)^2/(4a^3)$] as a free parameter whose value will eventually set the absolute temperature scale, then the wave vector $\boldsymbol{\tau}$ minimizing U_G can be determined for each set of parameters $\{J_0, J_1, J_2, \gamma_D\}$. The results for $\gamma_D = 0$ are shown in Fig. 2 in a pair of phase diagrams with $J_0 > 0$ (ferromagnetic) and $J_0 < 0$ (antiferromagnetic). The phases there are described by $\boldsymbol{\tau} = (h, k)$, referenced to the MnCl_2 sublattice. Representative values of η are given in the (η, η) region, where MnCl_2 GIC lies.

As γ_D increases, the range of stability of the (η, η) phase increases, and lines of constant η in this region are pushed to smaller J_1 and J_2 . Regions of stability for the observed GIC structure exist for some suitable γ_D for both $J_0 > 0$ and $J_0 < 0$, but only for $J_2 < 0$. The results demonstrate that at least three in-plane interaction terms are required to explain our data.

Numerical estimates are obtained by comparing the Curie-Weiss temperature, $\Theta = \frac{2}{3}S(S+1)6(J_0 + J_1 + J_2) = -5.9 \pm 0.5$ K, and the dipole prefactor, $\gamma_D = 12$ mK. Combining these two expressions gives the empirical constraint $\Delta E \equiv J_0 + J_1 + J_2 + 14.1\gamma_D = 0$. Because of uncertainties in Θ we consider all solutions for which $|\Delta E| < 0.3|J_0|$. With this constraint, there are no legitimate solutions for $J_0 < 0$ (the minimum $|\Delta E|$ there is $16|J_0|$). The range of solutions for $J_0 > 0$ is shown in Fig. 2, delimited by the dashed quadrilateral. Within most of the box, J_2 is stronger than both J_1 and J_0 . The first four lines of Table I give the parameter values for the four corners of the quadrilateral.

The strength of the third-neighbor term is surprising. Second-neighbor exchange couplings have occasionally been reported that are larger than those for first neighbors (e.g., MnO and NiO [15]). We are unaware of any other insulating magnet where the third-neighbor exchange is likely the strongest. In absolute scale, however, J_2 is at most about 0.3 K. What distinguishes MnCl_2 from other transition-metal dihalides [16,17] is an unusually small near-neighbor coupling, which gives more importance to the higher-order terms. For MnCl_2 GIC, J_0 is less than 100 mK, in contrast with 14 K for CoCl_2 [18] or 22 K for NiCl_2 [8].

Why is J_0 so small? The answer lies in a competition between superexchange mechanisms of nearly equal

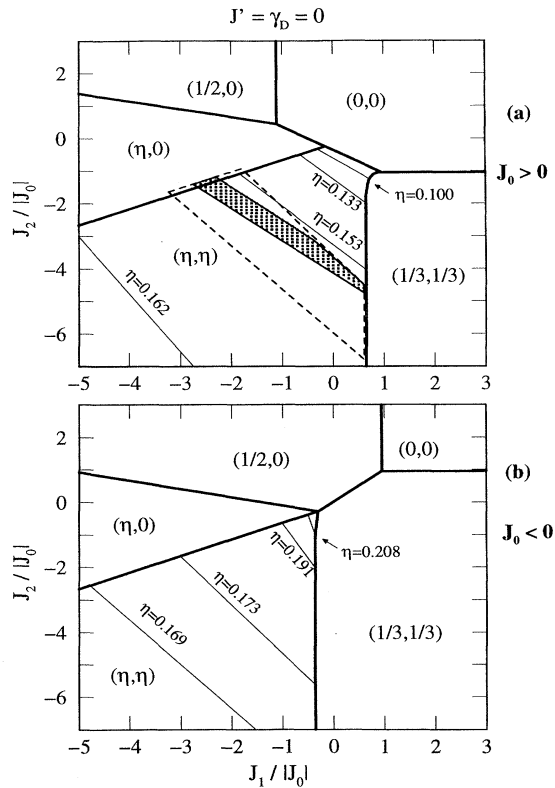


FIG. 2. $T = 0$ phase diagrams for $J' = 0$ and no dipole-dipole coupling: (top) ferromagnetic and (bottom) antiferromagnetic near-neighbor coupling. The modulation periodicity for MnCl_2 GIC occurs in the (η, η) phase at $\eta = 0.153$. Superimposed on the top panel are further constraints imposed by consideration of dipole-dipole coupling and interlayer exchange: The dashed quadrilateral denotes the range of solutions consistent with the high-temperature susceptibility data and the observed modulation wave vector. The smaller shaded region denotes the subset of these solutions for which the energy minimum would occur at the MnCl_2 modulation wave vector ($\eta = 0.10$) with the addition of a suitable J' .

strengths. The electron configuration of Mn^{2+} is given by $d_e^3 d_\gamma^2$, where the threefold d_e (t_{2g}) levels lie lower than the twofold d_γ (e_g) levels [see Fig. 3(a)]. Near-neighbor superexchange proceeds through two Mn^{2+} - Cl^- bonds which, because of the octahedral coordination, are nearly perpendicular to each other [16,17].

TABLE I. Representative solutions for MnCl_2 GIC low-temperature magnetic structure. The first four rows correspond to the four corners of the large quadrilateral in Fig. 2. The shaded region of Fig. 2, corresponding to self-consistent solutions for both the pristine and intercalation compounds, roughly spans the last two rows here.

J_1/J_0	J_2/J_0	γ_D/J_0	J_0 (mK)	J' -pris (K)
-3.1	-1.8	0.298	40	...
-1.9	-1.0	0.114	100	...
0.6	-6.8	0.390	30	...
0.6	-4.5	0.185	60	± 1.0
-2.5	-1.3	0.178	70	± 1.0

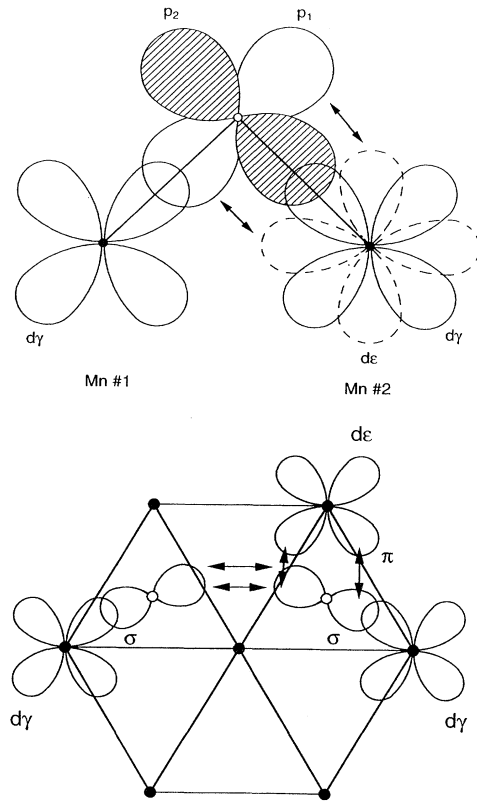


FIG. 3. (a) The near-neighbor superexchange, showing the competition between two mechanisms (as discussed in the text). (b) Projection onto the intercalate plane of the d and p orbitals of Mn^{2+} and Cl^- involved in the double-anion superexchange. J_1 requires one d_γ - p_σ and one d_e - p_π bond, while J_2 involves two d_γ - p_σ bonds.

In the formulation of Goodenough [16], three mechanisms come into play. The first, quasidirect exchange, favors antiferromagnetism; neighboring Mn^{2+} ions can share electrons only if their spins are antiparallel, since both d shells are half filled. The second mechanism involves partial p_σ - d_γ bond formation by transfer from the Cl^- to the Mn^{2+} of an electron, whose spin must be antiparallel to the Mn^{2+} spin. The electron is then replaced by one of like spin from the other Mn^{2+} via a p_π - d_e partial bond, leading again to antiferromagnetic correlations. In the third mechanism, electrons from the Cl^- are partially transferred to each of the neighboring Mn^{2+} ions simultaneously via two p_σ - d_γ bonds. Hund's first rule favors the spins remaining on the Cl^- to be aligned, giving a net ferromagnetic interaction between the Mn^{2+} spins. This mechanism becomes more important for shells half filled or more [16]; apparently for MnCl_2 GIC it narrowly wins out over the first two.

Given the small J_0 , a second question arises: Why is J_2 stronger than J_1 , or at least comparable to it? The answer is associated with the directionality of the bonds forming the superexchange pathways. Both J_1 and J_2 are mediated

through a double anion bridge involving the same anions, but the longer path involves no π bonds. As shown by a projection onto the a - b plane in Fig. 3(b), two p_{σ} - d_{γ} bonds are involved in the bridge for J_2 , whereas one of the bonds must be a p_{π} - d_{ϵ} bond for the bridge to J_1 .

There are important implications of this study to bulk MnCl_2 . Between T_{N1} and T_{N2} , a diffraction pattern was observed that, when projected onto the $(h, k, 0)$ plane, looks like the pattern in Fig. 1, except that \mathbf{k}_1 indexes to a commensurate value, $\text{Mn}(\frac{1}{10}, \frac{1}{10})$. The pattern was tentatively described by a 2×5 rectangular superstructure with three 120° twin domains. Below T_{N2} , each spot in the diffraction halo splits into two, rotated $\pm 11^\circ$ from the original spot.

Assuming that intercalation does not appreciably affect the exchange terms, the pristine MnCl_2 data supply a further constraint on the exchange parameters. For all points inside the dashed box in Fig. 2, we have calculated the minimum energy configuration as a function of interplanar coupling strength J' by Eq. (3). The shaded region in Fig. 2 is the subset of those parameters for which the energy minimum can be made to occur at $\text{Mn}(\frac{1}{10}, \frac{1}{10})$ by a suitable choice of J' . Inside this region, J' has a value of $-(16 \pm 3)|J_0|$ and $\gamma_D = (0.19 \pm 0.03)|J_0|$ (see Table I).

We expect our results to be relevant also to MnI_2 and MnBr_2 , which, like MnCl_2 , have layered structures [19]. It is probable that the magnetic structures for these compounds arise also from a competition between superexchange mechanisms of different signs and that higher-neighbor interactions are important (if not preeminent). Obtaining more precise estimates of the exchange parameters will require further study of the spin-wave dispersion by inelastic neutron scattering.

We thank H. Suematsu for providing us with single crystal Kish graphite, H. Zabel for initial support of this work, and D.A. Neumann for useful discussions. The work at SUNY-Binghamton was supported by NSF Grant No. DMR 9201656.

- [1] C. Starr, F. Bitter, and A.R. Kaufmann, *Phys. Rev.* **58**, 977 (1940).
- [2] R.B. Murray and L.D. Roberts, *Phys. Rev.* **100**, 1067 (1955); R.B. Murray, *ibid.* **100**, 1071 (1955); **128**, 1570 (1962).
- [3] M.K. Wilkinson *et al.*, Oak Ridge National Laboratory Report No. ORNL-2430, 65 (1957); Report No. ORNL-2501, 37 (1958).
- [4] W.F. Giaque *et al.*, *J. Chem. Phys.* **42**, 1 (1965); M. Regis and Y. Farge, *J. Phys. (Paris)* **37**, 627 (1976); A.F. Lorenko *et al.*, *Sov. Phys. JETP* **62**, 714 (1985).
- [5] J.W. Stout and R.C. Chisholm, *J. Chem. Phys.* **36**, 979 (1962).
- [6] M.K. Wilkinson *et al.*, *Phys. Rev.* **113**, 497 (1959).
- [7] R.C. Chisholm and J.W. Stout, *J. Chem. Phys.* **36**, 972 (1962).
- [8] P.A. Lindgård *et al.*, *J. Phys. C* **8**, 1059 (1975).
- [9] D.G. Wiesler *et al.*, *Phys. Rev. B* **34**, 7951 (1986).
- [10] K. Koga and M. Suzuki, *J. Phys. Soc. Jpn.* **53**, 786 (1984).
- [11] O. Gonzalez *et al.*, *Solid State Commun.* **51**, 499 (1984); Y. Kimishima *et al.*, *J. Phys. C* **19**, L43 (1986); M. Suzuki *et al.*, *J. Magn. Magn. Mater.* **54-57**, 1275 (1986).
- [12] This temperature is sufficiently low to be taken as representative of $T = 0$, as we will show in a future publication detailing the temperature dependence of the scattering.
- [13] H. Shiba and M. Suzuki, *J. Phys. Soc. Jpn.* **51**, 3488 (1982).
- [14] We have also considered a stripe-domain model, such as proposed by Wilkinson *et al.* for pristine MnCl_2 , by adding appropriate odd harmonics to \mathbf{S}_q . Because the higher harmonics are much weaker than the fundamental, our results are largely insensitive to this difference.
- [15] M.E. Lines and E.D. Jones, *Phys. Rev.* **139**, A1313 (1965); M.T. Hutchings and E.J. Samuelsen, *Solid State Commun.* **9**, 1011 (1971).
- [16] J.B. Goodenough, *Magnetism and the Chemical Bond* (Interscience Publishers, New York, 1963).
- [17] J. Kanamori, *J. Phys. Chem. Solids* **10**, 87 (1959).
- [18] M.T. Hutchings, *J. Phys. C* **6**, 3143 (1973).
- [19] E.O. Wollan *et al.*, *Phys. Rev.* **110**, 638 (1958); J.W. Cable *et al.*, *ibid.* **125**, 1860 (1962).